

Paramagnetic NMR Spectroscopy and Coordination Structure of Cobalt(II) Cys112Asp Azurin

Mario Piccioli,[†] Claudio Luchinat,^{*,‡} Tadashi J. Mizoguchi,[§] Benjamin E. Ramirez,[§] Harry B. Gray,^{*,§} and John H. Richards^{*,§}

Department of Chemistry, University of Florence, Via G. Capponi 7, 50121 Florence, Italy, Institute of Agricultural Chemistry, University of Bologna, Viale Berti Pichat 10, 40127 Bologna, Italy, and Beckman Institute, California Institute of Technology, Pasadena, California 91125

Received October 6, 1994[⊗]

Paramagnetic ¹H-NMR spectra of Co(II)-substituted Cys112Asp azurin from *Pseudomonas aeruginosa* have been analyzed and compared with those of the Co(II) wild-type (WT) protein. Hyperfine-shifted signals (including Asp112 β-CH₂ signals in the mutant as well as previously unobserved Cys112 β-CH₂ signals in WT) from all the metal-coordinated residues have been detected and unambiguously assigned. Notably, the spectra indicate that very little if any unpaired spin density is located on the Met121 protons in the Cys112Asp protein. A computer-generated model of the mutant Co(II) structure consistent with electronic absorption as well as the NMR data includes a Gly45 carbonyl, His46, an unusually coordinated Asp112, and His117 in the ligation sphere.

Introduction

The distinctive spectroscopic properties of the blue copper in *Pseudomonas aeruginosa* azurin¹ are lost when the cysteine at position 112 is replaced by aspartic acid (Cys112Asp).² However, the Cys112Asp mutant retains the ability to bind both Cu(II) and Co(II) strongly, ostensibly utilizing aspartate as a substitute for the cysteine thiolate in the binding site.² To examine the question directly in the Co(II) derivative of Cys112Asp azurin, we have turned to paramagnetic ¹H-NMR spectroscopy, which has been shown to be a powerful tool for the elucidation of active-site structures of Co(II) proteins.³ Our NMR studies have confirmed that aspartate is a ligand in the Cys112Asp mutant, and, together with computer-modeling experiments and electronic spectroscopic data, have shed additional light on the site coordination geometry.

Experimental Section

DNA and Mutagenesis. Standard techniques were employed throughout this work.⁴ A synthetic gene was used for the heterologous expression of *Pseudomonas aeruginosa* azurin in *Escherichia coli*.⁵ The single-site mutation, Cys112Asp, was made by oligonucleotide-directed mutagenesis using the Muta-Gene Phagemid *In Vitro* Mutagenesis Kit (Bio-Rad).² Gene sequences were confirmed by the chain-termination method using Sequenase Version 2.0 (United States Biochemical).

Protein Expression and Purification. Azurins were expressed using the pET System (Novagen). The appropriate genes were subcloned into the pET-9a expression vector and subsequently intro-

duced into the *E. coli* host strain BL21(DE3). A typical protein preparation involved growing a 4 L culture in 2xYT media at 30 °C. Protein synthesis was induced with the addition of 0.75% IPTG when the optical density of the culture at 600 nm reached ~1.5; the culture was incubated at 30 °C for another 5–6 h. The cell paste was isolated by centrifugation (4000g) at 4 °C in 6 × 250 mL centrifuge bottles. The cells were resuspended with gentle shaking at room temperature in 6 × 60 mL of 20% sucrose/30 mM Tris-HCl/1 mM sodium EDTA (pH 8). Once resuspended, the cell paste was reisolated by centrifugation (10000g) at 4 °C. The periplasmic fraction was released into solution by osmotic shock⁶ with the addition of 6 × 60 mL of ice-cold 4 mM NaCl followed by vigorous resuspension. These suspensions were shaken gently at 4 °C for 8–12 h. This mixture was centrifuged (4000g) at 4 °C, and the supernatant was collected without concern for contamination from some cellular debris. To the supernatant was added slowly 1/10 volume of 0.5 M sodium acetate (pH 4.1) with stirring at 4 °C. The resulting white precipitate was removed by centrifugation (10000g) at 4 °C, and the clear supernatant containing crude azurin was saved for further purification.

To the crude azurin solution was added sodium EDTA to 10 mM. The resulting solution was allowed to stand at 4 °C for at least 1 week. The protein solution was concentrated, and simultaneously, the buffer composition changed to 10 mM DEA-HCl (pH 8.8) using a stirred ultrafiltration unit with a YM3 membrane (Amicon). Azurin was purified from this solution by FPLC on a Mono Q column (Pharmacia) using a linear NaCl gradient. Two different azurin fractions were obtained. The lack of color and nonreconstitutability of the first fraction suggested that it was mostly Zn(II)-substituted azurin,⁷ while the second fraction corresponded to the apoprotein. This first fraction could be converted to the apo form upon incubation in 0.1 M sodium acetate/0.1 M thiourea/10 mM sodium EDTA (pH 4.5) at room temperature. The apoprotein was repurified before reconstitution. The typical yield of purified azurin was ~30 mg/L of culture.

The Co(II)-substituted azurins were made by the addition of a moderate excess of CoCl₂(aq) to a buffered solution of apoprotein. The reconstitution reaction was complete within several minutes. Wild-type (WT) Co(II) azurin appears light blue, while Co(II) Cys112Asp azurin is light purple. The Co(II) azurins were purified by FPLC (same conditions as described above) before further use.

Spectroscopic Measurements. Concentrated protein samples for spectroscopic measurements were obtained using Centricon-10 con-

[†] University of Florence.

[‡] University of Bologna.

[§] California Institute of Technology.

[⊗] Abstract published in *Advance ACS Abstracts*, January 1, 1995.

- (1) (a) Sykes, A. G. *Adv. Inorg. Chem.* **1991**, *36*, 377–408. (b) Adman, E. T. *Adv. Protein Chem.* **1991**, *42*, 145–197. (c) Solomon, E. I.; Baldwin, M. J.; Lowery, M. D. *Chem. Rev.* **1992**, *92*, 521–542.
- (2) Mizoguchi, T. J.; Di Bilio, A. J.; Gray, H. B.; Richards, J. H. *J. Am. Chem. Soc.* **1992**, *114*, 10076–10078.
- (3) Bertini, I.; Turano, P.; Vila, A. J. *Chem. Rev.* **1993**, *93*, 2833–2932.
- (4) Sambrook, J.; Fritsch, E. F.; Maniatis, T. *Molecular Cloning: A Laboratory Manual*, 2nd ed.; Cold Spring Harbor Laboratory: Cold Spring Harbor, NY, 1989.
- (5) (a) Chang, T. K.; Iverson, S. A.; Rodrigues, C. G.; Kiser, C. N.; Lew, A. Y. C.; Germanas, J. P.; Richards, J. H. *Proc. Natl. Acad. Sci. U.S.A.* **1991**, *88*, 1325–1329. (b) Germanas, J. P.; Di Bilio, A. J.; Gray, H. B.; Richards, J. H. *Biochemistry* **1993**, *32*, 7698–7702.

(6) Neu, H. C.; Heppel, L. A. *J. Biol. Chem.* **1965**, *240*, 3685–3692.

(7) Nar, H.; Huber, R.; Messerschmidt, A.; Filipponi, A. C.; Barth, M.; Jaquinod, M.; van de Kamp, M.; Canters, G. W. *Eur. J. Biochem.* **1992**, *205*, 1123–1129.

centrator units (Amicon). Reported pH values were not corrected for the deuterium isotope effect.

NMR spectra were recorded on a Bruker AMX600 spectrometer operating at a magnetic field of 14.1 T or on a Bruker MSL200 at 4.7 T. 1D experiments were performed using the superWEFT pulse sequence ($180^\circ - \tau - 90^\circ$).⁸ NMR spectra were calibrated by assigning the H₂O or the residual HDO signal a chemical shift of 4.81 ppm from DSS (298 K). 1D NOE difference spectra were recorded using previously reported methodology.⁹ 2D NOESY experiments were recorded in the phase-sensitive TPPI mode.¹⁰ In order to detect connectivities among hyperfine-shifted, fast-relaxing signals, 1024 × 512 data-point matrices were collected over a 100-kHz spectral width. Mixing and recycle delays were 6 and 120 ms, respectively. To investigate the spectral region between -10 and +20 ppm, NOESY experiments were recorded using 2048 × 1024 data points over a 20-kHz spectral width. Mixing and recycle delays were 15 and 580 ms, respectively. To suppress the strong solvent signal, presaturation was used during both mixing and recycle delays. A COSY experiment, recorded in the magnitude mode, was acquired over a 20-kHz spectral width. A total of 2048 × 512 data points were acquired using 480 ms of recycle delay. The same experiment was also performed using 512 × 180 data points with 115 ms of recycle delay. All 2D NOESY data were processed using a shifted ($\pi/2$ or $\pi/3$) sine-squared weighting function in both dimensions prior to Fourier transformation. An unshifted sine-squared weighting function was used in processing 2D COSY data.

Absorption spectra were recorded on a modified Cary 14 spectrophotometer.

Computer Modeling. Azurin structures were modeled by employing the BIOGRAF simulation package (Molecular Simulations) based on the crystal structure coordinates of *P. aeruginosa* azurin (PDB code 4azu)¹¹ in which the copper ion was removed and all hydrogen atoms were added. All calculations were done using POLARIS AminoLib charges¹² and DREIDING II force-field parameters.¹³ Note that the Cys112 thiolate was protonated to the corresponding thiol prior to minimization. The apo-WT azurin crystal structure was minimized with all atoms moveable by five steps of deepest-descent minimization followed by 200 steps of conjugate-gradient minimization. Thereafter, all mutants that were built converged within 100 steps of conjugate-gradient minimization. Cys112Asp azurin was constructed by replacing the sulfhydryl group of Cys112 in the calculated apo-WT azurin structure with a randomly oriented carboxylate group.

Results and Discussion

The 200-MHz ¹H-NMR spectra of both the Co(II)-substituted WT and Cys112Asp azurins show a number of hyperfine-shifted signals (Figure 1). Most of the WT azurin signals have been observed and assigned previously.¹⁴ The two WT azurin signals *a* and *b* (Figure 1A,B), previously unobserved,¹⁵ can be assigned to the β -CH₂ protons of Cys112. β -CH₂ protons of coordinated cysteines are always found far downfield in Co(II)-substituted metalloproteins.¹⁶ Their large hyperfine shifts confirm regular

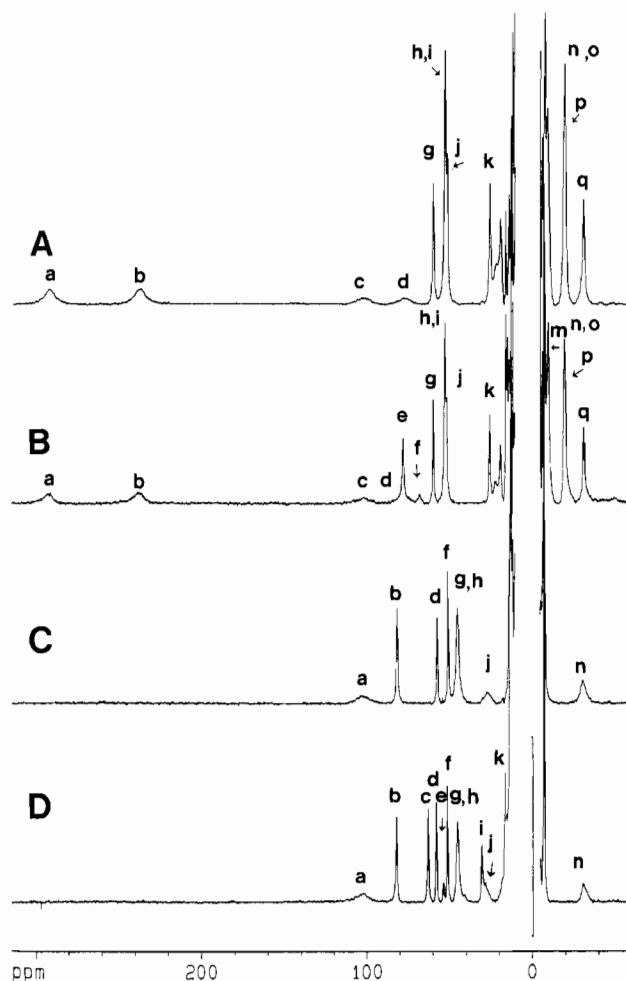


Figure 1. 200-MHz ¹H-NMR spectra (298 K): Co(II) WT azurin (pH 8.0) in D₂O solution (A) and H₂O solution (B); Co(II) Cys112Asp azurin (pH 7.0) in D₂O solution (C) and H₂O solution (D).

coordination of Cys112 to the Co(II) ion. These signals are not present in the Asp112 mutant (Figure 1C,D).

The assignment of histidine ring protons can be achieved through NOE and NOESY data on H₂O and D₂O samples. Comparison of the H₂O and D₂O NMR spectra of both the WT and mutant proteins reveals the disappearance of WT signals *e* and *f* (Figure 1B,A) and mutant signals *c* and *e* (Figure 1D,C), all of which can be assigned to exchangeable imidazole NH protons. WT signal *f* and mutant signal *e* have fractional intensities due to partial saturation from solvent but gain full intensity at lower pH (data not shown). From NOE and NOESY experiments, WT signal *e* is dipole-coupled to signal *h* and signal *f* is dipole-coupled to signal *g* (data not shown), as already reported.¹⁴ Likewise, in the mutant, signal *c* is dipole-coupled to signal *f* and signal *e* is dipole-coupled to signal *d*. Figure 2 shows the region of the NOESY spectrum for the Cys112Asp derivative where the connectivities *c*-*f* and *d*-*e* are observed. In line with previous work,¹⁴ the *e*-*h* and *f*-*g* pairs in the WT protein are assigned to H^{ε2}-H^{δ2} pairs of two coordinated histidines, and the same assignment is made for the *c*-*f* and *d*-*e* pairs in the mutant.

The sequence-specific assignment is facilitated by the observation that the H^{ε2} proton of His117 is solvent-exposed while that of His46 is not. The fractional intensity of WT signal *f* and mutant signal *e* at pH 7.0 indicates relatively high solvent-exchange rates. Therefore, WT pair *e*-*h* and mutant pair *c*-*f* are assigned to His46 whereas WT pair *f*-*g* and mutant pair *d*-*e* are assigned to His117. The chemical shifts of these signals

- (8) Inubushi, T.; Becker, E. D. *J. Magn. Reson.* **1983**, *51*, 128-133.
- (9) Banci, L.; Bertini, I.; Luchinat, C.; Piccioli, M.; Scozzafava, A.; Turano, P. *Inorg. Chem.* **1989**, *28*, 4650-4656.
- (10) Marion, D.; Wüthrich, K. *Biochem. Biophys. Res. Commun.* **1983**, *113*, 967-974.
- (11) Nar, H.; Messerschmidt, A.; Huber, R.; van de Kamp, M.; Canters, G. W. *J. Mol. Biol.* **1991**, *221*, 765-772.
- (12) Lee, F. S.; Chu, Z. T.; Warshel, A. *J. Comput. Chem.* **1993**, *14*, 161-185.
- (13) Mayo, S. L.; Olafson, B. D.; Goddard, W. A., III. *J. Phys. Chem.* **1990**, *94*, 8897-8909.
- (14) Moratal, J.-M.; Salgado, J.; Donaire, A.; Jiménez, H. R.; Castells, J. *Inorg. Chem.* **1993**, *32*, 3587-3588.
- (15) Signals *a*, *b*, *c* (Figure 1A,B) are located beyond the scale of the NMR spectra reported in ref 14.
- (16) (a) Bertini, I.; Gerber, M.; Lanini, G.; Luchinat, C.; Maret, W.; Rawer, S.; Zeppezauer, M. *J. Am. Chem. Soc.* **1984**, *106*, 1826-1830. (b) Bertini, I.; Luchinat, C.; Messori, L.; Vařák, M. *J. Am. Chem. Soc.* **1989**, *111*, 7296-7300. (c) Moura, I.; Teixeira, M.; LeGall, J.; Moura, J. J. G. *J. Inorg. Biochem.* **1991**, *44*, 127-139.

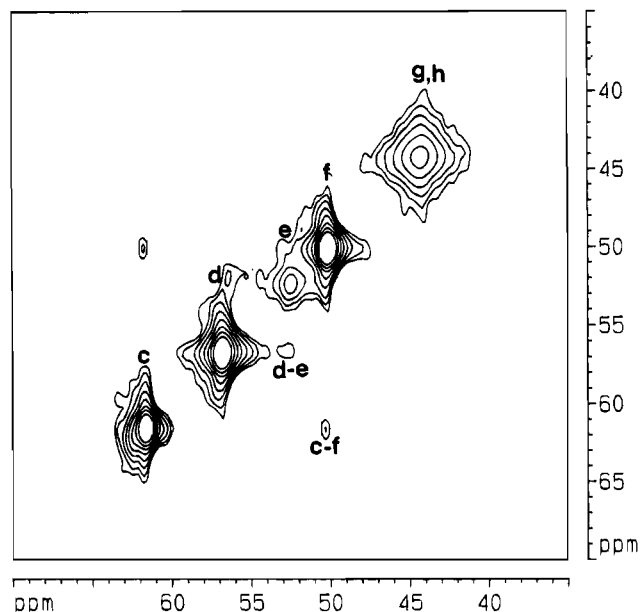


Figure 2. 600-MHz NOESY spectrum (298 K) of Co(II) Cys112Asp azurin (pH 7.2). The 35–70 ppm region is reported. Cross peaks between signals *c* and *f* and between signals *d* and *e* are observed. The cross peak between *d* and *e* is weaker than the other cross peak because signal *e* is of fractional intensity at this pH.

in both systems are all in the range (50–80 ppm) typical of ring protons of regularly coordinated histidines.¹⁷ The H^{ε1} protons are expected to yield much broader signals due to their ring positions adjacent to the coordinating N^{δ1} nitrogens. Possible candidates for these protons are WT signals *c* and *d* (previously unobserved)¹⁵ and mutant signals *a* and *j* (Figure 1). However, no connectivities could be detected from such broad signals to confirm this assignment. If the assignment is correct, the smaller shift of signal *j* for the mutant would be indicative of some difference in at least the pseudocontact contribution to the shift of this proton in the immediate vicinity of the metal ion.

There is a strong NOESY and COSY cross peak between WT signals *i* and *q* (data not shown), as observed previously.¹⁴ Despite their experiencing hyperfine shifts opposite in sign, they have been assigned as the α-CH₂ proton pair of Gly45. This assignment is confirmed by an NOE between signal *q* and the slowly exchangeable proton *m* (Figure 1B) assigned as the amide NH proton of Gly45. In the mutant protein, no similarly strong connectivities between upfield- and downfield-shifted signals are observed. However, strong NOESY and COSY connectivities typical of a geminal proton pair are detected between mutant signals *b* and *l*, both downfield, although one is much more shifted than the other (Figure 3).¹⁸ Figure 3B shows the –15 to +20 ppm region of the 1D NOE difference spectrum obtained upon saturation of mutant signal *b* in D₂O. In addition to the strong NOE to signal *l*, an NOE to signal *m* is also

observed. Mutant signal *b* experiences additional dipolar connectivities involving hyperfine-shifted signals. Figure 3A shows the 1D NOE difference spectra over the entire spectral window obtained upon irradiation of signal *b* in H₂O solution (trace a) and D₂O solution (trace b). In H₂O, two NOEs are observed with the exchangeable signals *i* and *k*. Inspection of the X-ray crystal structure of azurin¹¹ confirms that no other reasonable candidate exists for a hyperfine-shifted geminal proton pair close in space to hyperfine-shifted exchangeable protons. Therefore, we conclude that the *b*–*l* pair in the mutant must be assigned to the α-CH₂ protons of Gly45. Mutant signal *i* can then be assigned to the amide NH proton of His46 in view of its larger shift and signal *k* to the amide NH proton of Gly45 itself. In contrast to those of the analogous WT protons, the substantially different hyperfine shifts of some of the above protons indicate that, although they are coordinated in both cases, some differences may exist in the binding mode of the Gly45 carbonyl group. For example, a slightly shorter carbonyl–Co(II) bond in the mutant might significantly increase the downfield contact contribution to the shifts of both α-CH₂ protons of Gly45 and the amide NH proton of His46. Alternatively, a reduction in the upfield pseudocontact contribution from WT to mutant is possible.

Of the other hyperfine-shifted signals outside the diamagnetic region (Figure 1), we are left with signals *j*, *k*, *n*, *o*, *p* in WT and signals *g*, *h*, *n* in the mutant. There is little analogy between the two derivatives as far as these signals are concerned. Signals *g* and *h* in the mutant have shifts and line widths typical of β-CH₂ protons of a coordinated carboxylate residue (Figure 3A)¹⁹ and hence can be assigned to Asp112 coordinated regularly through at least one oxygen.

WT signals *j* and *p* have been assigned tentatively to the γ-CH₂ protons of Met121, with signals *n* and *o* attributed to the β-CH₂ protons.¹⁴ The NOE experiments performed upon saturation of the WT signals *a* and *b* (β-CH₂ protons of Cys112) allowed us to detect an NOE between signal *b* and at least one of the two unresolved signals *n* and *o* (Figure 4). Such an NOE is consistent with the proposed assignment¹⁴ of signals *n* and *o* to the β-CH₂ protons of Met121.

A crucial point for the assignment of Met121 signals would be the identification of the ε-CH₃ signal. As can be seen in Figure 5, WT signal *l* (of intensity 3), assigned previously as the ε-CH₃ protons of Met121,¹⁴ is dipolarly connected to signal *q* (H^α of Gly45). Signal *l* gives rise to three dipolar connectivities (Figure 6A, cross peaks 1–3) with signals belonging to the same spin pattern, as can be observed from the COSY experiment reported in Figure 6B. The signal at –4.8 ppm has intensity 3; the only residue with two methyl groups occurring at short distance from one of the H^α protons of Gly45 (signal *q*) is Leu86.¹¹ As signal *l* is much broader than the signal corresponding to the other methyl group, inspection of the X-ray structure¹¹ suggests the assignment of *l* to δ²-CH₃ of Leu86 (*i.e.*, the methyl group closer to the metal ion). This conclusion is supported by the network of interresidue connectivities (see caption to Figure 6) that involve Leu86 with Lys41 and Leu68. The COSY spectrum (Figure 6B) allows us to identify every resonance of Lys41, which, along with Leu86, is one of the residues close to the active site but not coordinated to the metal ion. All the signals of Lys41 experience a slight upfield pseudocontact shift (0 to 6 ppm). The signal of δ¹-CH₃ of Leu86 is also dipole–dipole coupled to another signal of a

(17) (a) Bertini, I.; Canti, G.; Luchinat, C.; Mani, F. *J. Am. Chem. Soc.* **1981**, *103*, 7784–7788. (b) Bertini, I.; Luchinat, C.; Piccioli, M. *Prog. Nucl. Magn. Reson. Spectrosc.* **1994**, *26*, 91–139.

(18) The spectrum of Co(II) Cys112Asp azurin at pH 5.5 (Figure 3A) is slightly different from the spectrum at pH 8.0 (Figure 1D). Indeed, some signals experience hyperfine-shift changes. In particular, signals *c*, *h*, and *i* move slightly downfield, sizably upfield, and slightly upfield, respectively, on decreasing the pH from 7.0 to 4.5. At intermediate pH values, both “high pH” and “low pH” signals are observed. Signals from the “high pH” form (the minor species at pH 5.5) are labeled with primes. The observation of two sets of signals at intermediate pH values demonstrates the presence of two pH-dependent species in equilibrium. The rate of chemical exchange between the two species is slow on the NMR time scale ($k_{ex} \leq 2 \times 10^3 \text{ s}^{-1}$).

(19) (a) Holz, R. C.; Que, L., Jr.; Ming, L.-J. *J. Am. Chem. Soc.* **1992**, *114*, 4434–4436. (b) Bertini, I.; Lanini, G.; Luchinat, C.; Messori, L.; Monnanni, R.; Scozzafava, A. *J. Am. Chem. Soc.* **1985**, *107*, 4391–4396.

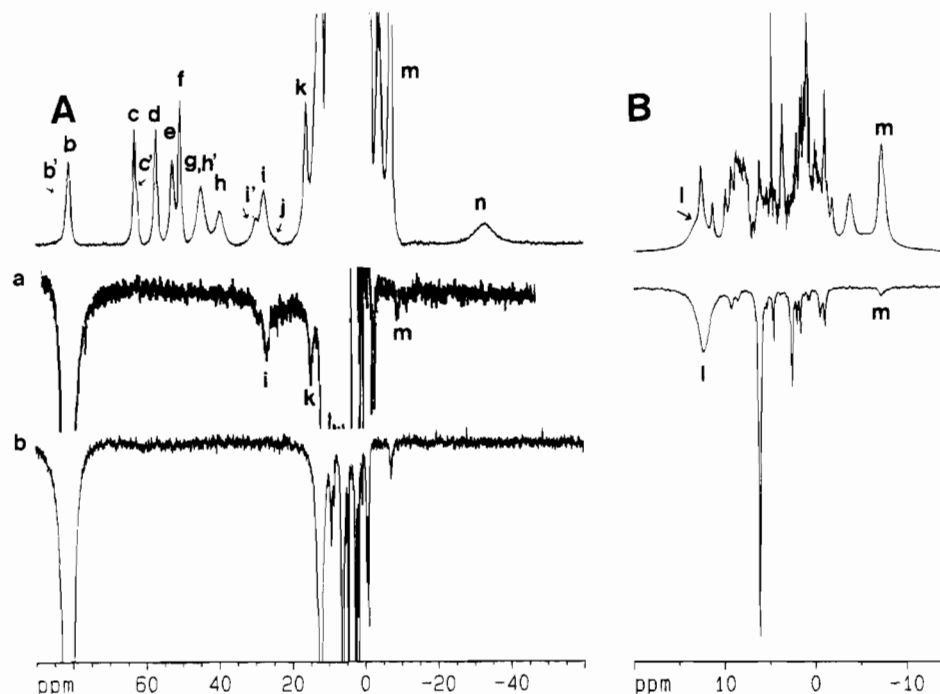


Figure 3. (A) 600-MHz 1D NOE difference spectra (298 K) obtained upon selective saturation of signal *b* of Co(II) Cys112Asp azurin (pH 5.5).¹⁸ Trace *a* is the 1D difference spectrum in H₂O, and trace *b* is the 1D difference spectrum in D₂O. Connectivities between signals *b* and two exchangeable signals *i* and *k* are observed. The reference spectrum is also given. (B) An expanded plot of the -15 to +20 ppm region of the difference spectrum of trace *b*, together with the reference spectrum in D₂O solution. Besides several other NOEs that are not discussed, a strong NOE is observed with broad signal *i* as well as a weak NOE with signal *m*, which corresponds to a methyl resonance.

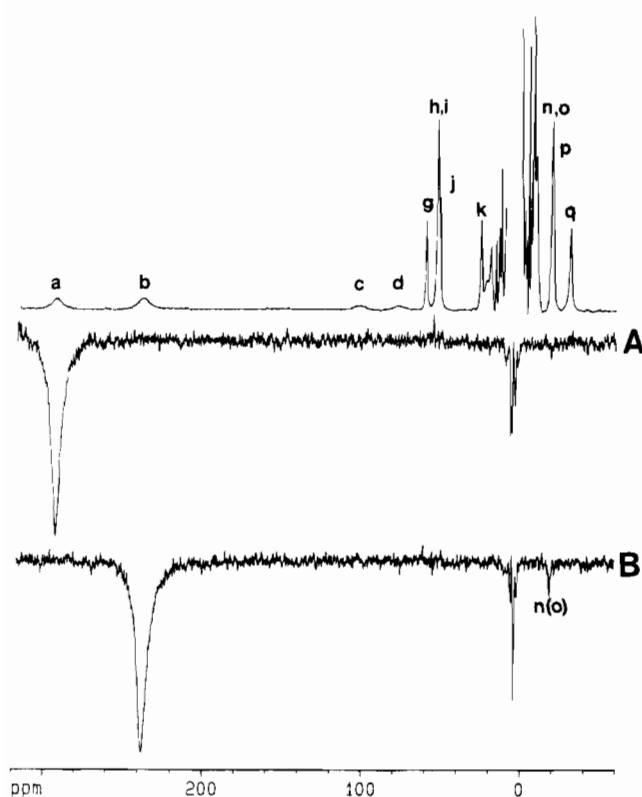


Figure 4. 200-MHz 1D NOE difference spectra (298 K) obtained upon selective saturation in D₂O solution (pH 8.0) of signals *a* (A) and *b* (B) of Co(II) WT azurin. An NOE with one of the two overlapped signals *n* and *o* is observed when signal *b* is saturated. The reference spectrum is also given.

methyl group that can be assigned on the basis of the X-ray structure¹¹ to Leu68. In summary, the NOESY and COSY maps (Figure 6) have allowed us to assign almost all the upfield-shifted signals (because of pseudocontact shifts) in the region

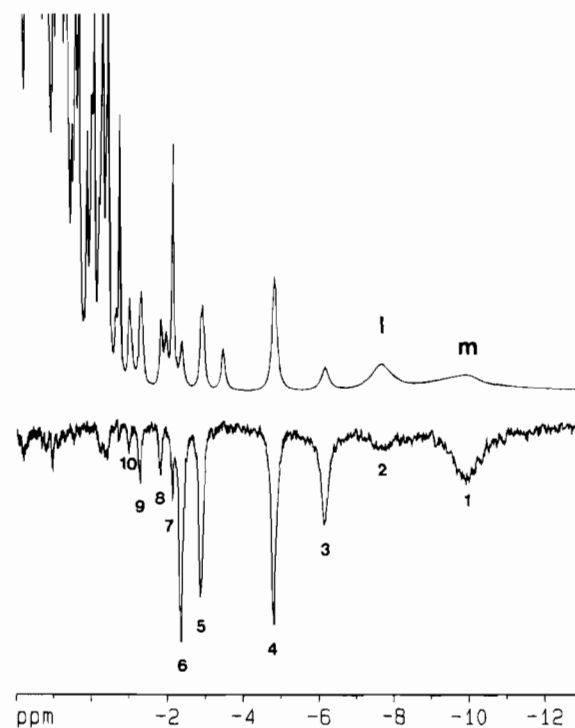


Figure 5. 600-MHz 1D NOE difference spectrum (298 K) obtained upon saturation of signal *q* in Co(II) WT azurin in H₂O solution (pH 7.2). The NOE peaks indicated with numbers are assigned (mainly on the basis of NOESY and COSY data in Figure 6) as follows: (1) NH-Gly45, (2) δ^2 -CH₃(Leu86), (3) H $^\alpha$ (Leu86), (4) δ^1 -CH₃(Leu86), (5) H $^{\gamma 1}$ (Lys41) and H $^\beta$ (Lys41), (6) H $^\alpha$ (Lys41), (7) δ -CH₃(Leu68), (8) H $^{\gamma 2}$ (Lys41), (9) H $^\beta$ (Lys41), (10) H $^\alpha$ (Lys41). Small cross peaks 7, 8, and 10 are likely due to spin diffusion. The reference spectrum in the -13 to +2 ppm region is also reported.

-14 to -0.3 ppm. The NOEs observed upon saturation of upfield signal *q* are all consistent with these assignments and are reported in the caption to Figure 5. In agreement with this

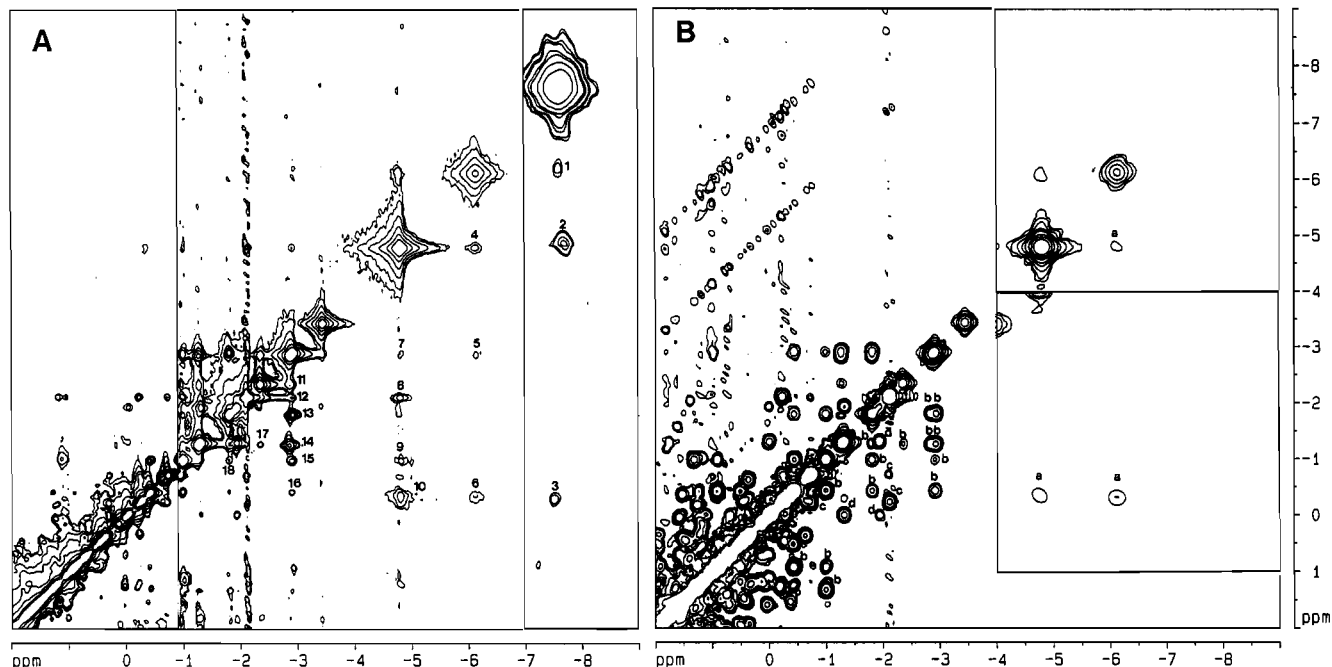


Figure 6. 600-MHz NOESY (A) and COSY (B) spectra (298 K) of Co(II) WT azurin in H₂O solution (pH 7.2) in the -9 to +2 ppm region. In the NOESY spectrum (A), cross peaks are labeled as follows: (1) δ^2 -CH₃(Leu86)-H ^{γ} (Leu86), (2) δ^2 -CH₃(Leu86)- δ^1 -CH₃(Leu86), (3) δ^2 -CH₃(Leu86)-H ^{β} (Leu86), (4) H ^{γ} (Leu86)- δ^1 -CH₃(Leu86), (5) H ^{γ} (Leu86)-H ^{γ} (Lys41), (6) H ^{γ} (Leu86)-H ^{β} (Leu86), (7) δ^1 -CH₃(Leu86)-H ^{γ} (Lys41), (8) δ^1 -CH₃(Leu86)- δ -CH₃(Leu68), (9) δ^1 -CH₃(Leu86)-H ^{δ} (Lys41), (10) δ^1 -CH₃(Leu86)-H ^{β} (Leu86), (11) H ^{β} (Lys41)-H ^{α} (Lys41), (12) H ^{γ} (Lys41)- δ -CH₃(Leu68), (13) H ^{γ} (Lys41)-H ^{γ} (Lys41), (14) H ^{β} (Lys41)-H ^{β} (Lys41), (15) H ^{γ} (Lys41)-H ^{δ} (Lys41), (16) H ^{γ} (Lys41)-H ^{δ} (Lys41), (17) H ^{α} (Lys41)-H ^{β} (Lys41), (18) H ^{δ} (Lys41)-H ^{γ} (Lys41). Cross peaks 5, 7, 8, 9 identify the connections of the spin systems of Leu86 to the spin system of Lys41 and to the spin system of Leu68. In the COSY spectrum (B), letters indicate cross peaks belonging to the same spin systems. The spin systems are labeled as follows: (a) Leu86, (b) Lys41, (c) Leu68. Cross peaks indicated with (d) belong to a spin system that does not give rise to any dipolar connectivity with H ^{α} of Gly45 or any other resonance of the above assigned residues. NOESY (A): A higher field threshold level was used for the contour plot of the left panel; the right panel was obtained upon Fourier transformation of a 512 \times 256 data-point matrix. COSY (B): The upper and lower right panels were obtained upon Fourier transformation of 600 \times 300 and 360 \times 180 data-point matrices, respectively.

reassignment of WT, the homologous methyl signal *m* in the mutant is dipolarly connected to signal *b* (H ^{α} of Gly45), as observed clearly from 1D NOE data (Figure 3). Such an NOE is definitely inconsistent with the assignment of signal *m* to the ϵ -CH₃ protons of Met121, but it is consistent with the assignment of *m* to one of the δ -CH₃ protons of Leu86. We conclude that the ϵ -CH₃ signal of Met121 is unobserved in both derivatives (it should fall in the diamagnetic region of the spectrum). Mutant signal *n* gives an NOE to signal *m*. From an inspection of the X-ray crystal structure,¹¹ a plausible candidate for signal *n* is one of the β -CH₂ protons of Phe114.

There are no hyperfine-shifted signals in the mutant that can be related to WT signals *j* and *p*. A possible explanation is that the mutant γ -CH₂ protons of Met121 also fall in the diamagnetic region. Such a decrease in the hyperfine shifts of the γ -CH₂ protons of Met121 could arise from the fact that the methionine sulfur atom is not coordinated to the Co(II) ion in the Cys112Asp mutant. The absence of the two upfield-shifted signals (\sim 10 ppm) in the mutant (signals *n* and *o* in WT) is consistent with this explanation. All of the above observations point to modest hyperfine shifts experienced by all protons of Met121 in the WT protein and even smaller shifts by those of the mutant protein. In light of the present finding of very large hyperfine shifts for the β -CH₂ protons adjacent to a regularly coordinated sulfur atom of Cys112, the most likely interpretation of the data is that Met121 is *at most* semicoordinated in the WT structure and essentially not coordinated in the mutant. The larger downfield shifts of the Gly45 α -CH and NH and His46 NH protons are consistent with this view of the Co(II) coordination environment in the Asp112 protein.

The electronic absorption spectra of Co(II)-substituted WT and Cys112Asp azurins are shown in Figure 7. The intensities

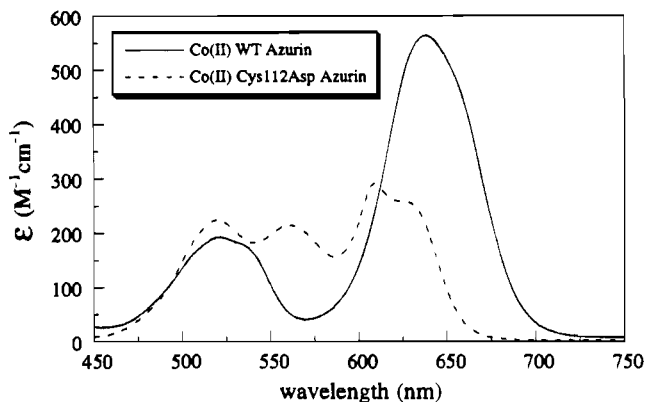


Figure 7. Absorption spectra of Co(II) WT and Cys112Asp azurins in aqueous 10 mM DEA-HCl/40 mM NaCl (pH 8.8) solutions at room temperature.

of the d-d bands in the spectrum of the WT protein fall in the range typical of distorted tetrahedral Co(II) ($\epsilon_{\max} > 250 \text{ M}^{-1} \text{ cm}^{-1}$).²⁰ It is likely that the pseudotetrahedral Co(II) coordination geometry is similar to that observed in the crystal structure of Zn(II) WT azurin, where the ligands are the Gly45 carbonyl and the side chains of His46, Cys112, and His117.⁷ Furthermore, the closely similar absorption spectra of the Co(II) derivative of Met121Leu azurin and WT protein suggest that

(20) (a) Rosenberg, R. C.; Root, C. A.; Wang, R.-H.; Cerdonio, M.; Gray, H. B. *Proc. Natl. Acad. Sci. U.S.A.* **1973**, *70*, 161-163. (b) Bertini, I.; Luchinat, C. In *Advances in Inorganic Biochemistry*; Eichhorn, G. L., Marzilli, L. G., Eds.; Elsevier: New York, 1984; Vol. 6, pp 71-111. (c) Bertini, I.; Gray, H. B.; Lippard, S. J.; Valentine, J. S. *Bioinorganic Chemistry*; University Science Books: Mill Valley, CA, 1994.

Met121 is not a ligand.²¹ Our NMR data, as well as results obtained in many earlier position 121 mutagenesis experiments,^{22,23} accord with this conclusion.

The d-d bands in the absorption spectrum of Co(II) Cys112Asp azurin are weaker than those of the Co(II) WT protein.²⁴ However, they are more intense than those generally found in five-coordinate Co(II) complexes ($50 < \epsilon_{\max} < 150 \text{ M}^{-1} \text{ cm}^{-1}$), being near the lower limit for distorted tetrahedral species ($\epsilon_{\max} > 250 \text{ M}^{-1} \text{ cm}^{-1}$).²⁰ As in the WT structure, the Gly45 carbonyl and the side chains of His46 and His117 coordinate the Co(II) ion. In order to assess the possible bonding modes of the Asp112 carboxylate group, a computer model of the active site was generated.

It has been shown that the structures of the apo and Cu(II) forms of WT azurin are nearly superposable,²⁵ and in terms of protein structure, a cysteine to aspartate change within the active site is a relatively conservative replacement with respect to the apo protein. Therefore, we propose that the calculated positions of the active-site side chains of apo-Cys112Asp azurin will not only be a valid approximation but also correspond to a reasonable model of the structure of the binding site of the Cu(II) or Co(II) derivative. Our minimized apo-WT azurin structure has an rmsd overlap²⁶ of $\sim 1.5 \text{ \AA}$ with the crystal structure, and the displacements of the copper-site ligands are similar to those reported for the crystal structure of apo-WT azurin.²⁵ The positions of the native copper ligands of all the calculated structures are nearly superposable.

According to this model, the Asp112 carboxylate group can adopt several reasonable conformations with respect to rotations about its $C^{\beta}-C^{\gamma}$ bond; monodentate or bidentate coordination can apparently be accommodated depending upon its orientation in the active site. A minimized structure of the metal-binding

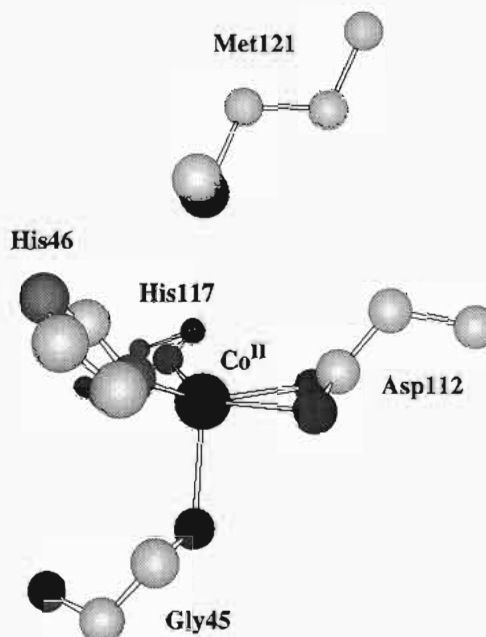


Figure 8. Computer-generated model of the active-site structure of Co(II) Cys112Asp azurin. The Co(II) ion was added manually to the minimized apoprotein structure. Reasonable bond distances could be achieved between the Co(II) center and the Gly45 carbonyl (2.3 Å), N^δ(His46) (2.1 Å), O^{δ1}(Asp112) (2.1 Å), O^{δ2}(Asp112) (2.5 Å), and N^δ(His117) (2.1 Å). In this model, the Co(II)-S^δ(Met121) distance is 3.7 Å.

site with the carboxylate group in a potentially bidentate binding mode is shown in Figure 8. Reasonable bond distances ($\sim 2 \text{ \AA}$) can be achieved from the Gly45 carbonyl, His46, and His117 to the metal center. Interestingly, the Asp112 carboxylate group can be positioned in such a way that both oxygens are located within reasonable bonding distances but in which one is significantly closer than the other. This model, intermediate between four- and five-coordination, suggests the existence of a bent bond²⁷ between Co(II) and the carboxylate, owing to the constraints placed on the 112 side chain by the global fold of the protein.²⁸ The apparent movement of the Co(II) ion away from Met121 toward the Gly45 carbonyl is not surprising, because the Asp oxygen donor atoms should harden the Co(II) center.²⁹ Thus, the Co(II) ion in the mutant will have greater affinity for the Gly45 carbonyl oxygen than for the softer sulfur atom of Met121.

Acknowledgment. We thank Ivano Bertini for many helpful discussions. This work was supported by the National Institutes of Health.

IC941148K

- (21) Di Bilio, A. J.; Chang, T. K.; Malmström, B. G.; Gray, H. B.; Karlsson, B. G.; Nordling, M.; Pascher, T.; Lundberg, L. G. *Inorg. Chim. Acta* **1992**, *198*, 198–200, 145–148.
- (22) (a) Karlsson, B. G.; Aasa, R.; Malmström, B. G.; Lundberg, L. G. *FEBS Lett.* **1989**, *253*, 99–102. (b) Karlsson, B. G.; Nordling, M.; Pascher, T.; Tsai, L. C.; Sjölin, L.; Lundberg, L. G. *Protein Eng.* **1991**, *4*, 343–349. (c) Pascher, T.; Karlsson, B. G.; Nordling, M.; Malmström, B. G.; Vännegård, T. *Eur. J. Biochem.* **1993**, *212*, 289–296. (d) Murphy, L. M.; Strange, R. W.; Karlsson, B. G.; Lundberg, L. G.; Pascher, T.; Reinhammar, B.; Hasnain, S. S. *Jpn. J. Appl. Phys.* **1993**, *32*, 561–563. (e) Murphy, L. M.; Strange, R. W.; Karlsson, B. G.; Lundberg, L. G.; Pascher, T.; Reinhammar, B.; Hasnain, S. S. *Biochemistry* **1993**, *32*, 1965–1975. (f) Farver, O.; Skov, L. K.; Pascher, T.; Karlsson, B. G.; Nordling, M.; Lundberg, L. G.; Vännegård, T.; Pecht, I. *Biochemistry* **1993**, *32*, 7317–7322. (g) Strange, R. W.; Murphy, L.; Karlsson, B. G.; Lindley, P. F.; Lundberg, L. G.; Reinhammar, B.; Hasnain, S. S. *Acta Crystallogr., Sect. D* **1994**, *50*, 37–39.
- (23) Wutke, D. S.; Gray, H. B. *Curr. Opin. Struct. Biol.* **1993**, *3*, 555–563.
- (24) The molar extinction coefficients for the d-d bands are larger than previously published values;² they were redetermined for both the Co(II) WT and Cys112Asp azurins by titrating purified apoprotein samples with a standardized solution of Co(II). Underestimation of extinction coefficients in azurins may arise in part from contamination from the colorless Zn(II) derivative.
- (25) Nar, H.; Messerschmidt, A.; Huber, R.; van de Kamp, M.; Canters, G. W. *FEBS Lett.* **1992**, *306*, 119–124.
- (26) Overlap included all non-hydrogen main-chain and side-chain atoms.

(27) For a discussion of metal-carboxylate bonds in proteins, see: Glusker, J. P. *Adv. Protein Chem.* **1991**, *42*, 1–76.

(28) We cannot exclude the possibility that Co(II) is in fast exchange between 4- and 5-coordinate geometries.

(29) Pearson, R. G. *Inorg. Chem.* **1988**, *27*, 734–740.